

**Double Periodicity and Frequency-Locking
in the Langford Equation**

Short running title:

Double Periodicity in the Langford Equation

Makoto Umeki

E-mail address: umeki@phys.s.u-tokyo.ac.jp

Department of Physics, Graduate School of Science

University of Tokyo, 7-3-1 Hongo, Bunkyo-ku, Tokyo 113-0033

Abstract

The bifurcation structure of the Langford equation is studied numerically in detail. Periodic, doubly-periodic, and chaotic solutions and the routes to chaos via coexistence of double periodicity and period-doubling bifurcations are found by the Poincaré plot of successive maxima of the first mode x_1 . Frequency-locked periodic solutions corresponding to the Farey sequence F_n are examined up to $n = 14$. Period-doubling bifurcations appears on some of the periodic solutions and the similarity of bifurcation structures between the sine-circle map and the Langford equation is shown. A method to construct the Poincaré section for triple periodicity is proposed.

Keywords: bifurcation, chaos, double periodicity, Langford equation

1 Introduction

A quasi-periodicity route to turbulence due to Ruelle and Takens [7] is that transition could occur via three successive Hopf bifurcations, leading from a fixed point to a limit cycle, then to a torus and finally to a 3-torus. On the other hand, double periodicity is considered to be well modeled by the one dimensional sine-circle map, which indicates that frequency-locking and periodic solutions appear as the nonlinear parameter increases. Therefore, it is a natural question what actually happens on attractors of a simple set of ordinary differential equations (ODEs) having double periodicity, like the Langford equation [4–6]. Similar numerical studies have been done for the five dimensional ODEs modeling magnetoconvection [1, 2] and the six dimensional ODEs of the Gledzer shell model of turbulence [8]. In the latter case the parameter to be changed is the viscosity, or equivalently, the Reynolds number. Both studies show a bifurcation structure very similar to that of the sine-circle map, although triple periodicity is stated based on the numerically obtained Lyapunov exponents in [2]. The presented results correspond to a detailed study that extends Langford [4–6].

In Section 2, a method to construct the three dimensional Poincaré section is proposed. For triple periodicity expected by Ruelle and Takens [7], points lie on a surface. Frequency-locked double periodicity indicates points on a closed curve embedded on the surface. Section 3 gives the Langford equation with an explanation of the evolution of the energy and selected parameters. In Section 4, numerical results of bifurcation structures of the equation are shown. It is confirmed that, instead of triple periodicity, we have double periodicity, frequency-locking and period-doubling bifurcations. The structure is very complicated; frequency-locking corresponding to the Farey sequence with the index up to 14 is confirmed, and plural sequences of the period-doubling bifurcations are observed. Summary and further possibilities to explore complexity of dynamical systems modeling fluid dynamics and other high dimensional systems with the presented approach are described in Conclusions.

2 Triple periodicity

As a typical example of triple periodicity, we consider the following function which is a sum of three sinusoidal functions of t ;

$$x(t; a, \omega) = \sin t + \sin \pi t + a \sin \omega t. \quad (1)$$

A standard method to construct the Poincaré map used in [1,8] is to seek for successive local maxima x_n of $x(t)$. Then we let $z_n = x_n + ix_{n+1}$ and $\theta_n = (2\pi)^{-1} \text{Arg}(z_n) \pmod{1}$. For double periodicity, θ_n obeys the generalized sine-circle map [8], which gives a curve on the (θ_n, θ_{n+1}) plane. Similarly, we can anticipate a surface in the $(\theta_n, \theta_{n+1}, \theta_{n+2})$ space. To check this analogy, we show the Poincaré plot of Eq. (1) in the time interval $0 < t < 5000$ for double periodicity $a = 0$ in Figure 1, triple periodicity $a = 0.5, \omega = \sqrt{2}$ in Figure 2, and frequency-locked double periodicity $a = 0.5, \omega = 1.4$ in Figure 3. Points lie on a curve in Figure 1 (a) and on a torus in Figure 2 (a), whose three dimensional structure can be viewed by a new 3D graphics function in *Mathematica* 6. The latter indicates a possibility that θ_{n+2} can be expressed by a function of θ_n and θ_{n+1} . This Poincaré plot will give a method to identify triple periodicity among complicated time series of general numerical or observed data.

We have 5:7 frequency-locking in the case of Figure 3. Correspondingly, points are again on a curve, which is more complicated than that in Figure 1. Actual data may contain higher harmonics in Eq. (1) but the qualitative behavior can be expected to be similar.

3 The Langford Equation

The Langford equation is the set of three ordinary differential equations for $x_i(t)$, $i = 1, 2, 3$, given as follows:

$$\frac{dx_1}{dt} = \dot{x}_1 = (x_3 - b)x_1 - cx_2, \quad (2)$$

$$\frac{dx_2}{dt} = \dot{x}_2 = cx_1 + (x_3 - b)x_2, \quad (3)$$

$$\begin{aligned} \frac{dx_3}{dt} = \dot{x}_3 = & d + ax_3 - \frac{x_3^3}{3} \\ & -(x_1^2 + x_2^2)(1 + fx_3) + ex_3x_1^3. \end{aligned} \quad (4)$$

The temporal evolution of the *energy* defined by $E = (1/2) \sum_{i=1}^3 x_i^2$ is given by

$$\frac{dE}{dt} = dx_3 + ax_3^2 - \frac{x_3^4}{3} - (b + fx_3^2)(x_1^2 + x_2^2) + ex_3^2x_1^3. \quad (5)$$

The set of the parameters fixed in this paper is borrowed from [6] as

$$(a, b, c, d, f) = (1, 0.7, 3.5, 0.6, 0.25), \quad (6)$$

and e is the changing parameter. Because $b > 0$ and $f > 0$, the right hand side of (5) becomes negative if E is sufficiently large for $e = 0$, leading to the proof that the solution is finite. If $e \neq 0$, the finiteness of the solution is unknown but supported by the numerical solution for small e .

The contraction rate of the volume element in the phase space is given by

$$\frac{\partial \dot{x}_1}{\partial x_1} + \frac{\partial \dot{x}_2}{\partial x_2} + \frac{\partial \dot{x}_3}{\partial x_3} = -x_3^2 + 2x_3 - 2b + a - f(x_1^2 + x_2^2) + ex_1^3. \quad (7)$$

It depends on the position in the phase space. If $e = 0$, it becomes negative for sufficiently large values of E since f is positive and the quadratic terms become dominant.

4 Bifurcation Structure

Before we show numerical results of the Langford equation, it is useful to review the bifurcation structure of the sine-circle map:

$$\theta_{n+1} = f(\theta_n) = \theta_n + \Omega + \frac{K}{2\pi} \sin(2\pi\theta_n), \quad (\text{mod } 1). \quad (8)$$

In order to compare the diagram of (8) with that of the Langford equation, the parameter Ω and K are parametrized as

$$\Omega = 0.5(1 + \alpha), \quad K = 4\alpha. \quad (9)$$

The initial condition is $\theta_1 = 0$, $0 < \alpha < 1$, $\Delta\alpha = 0.001$, the total iteration is 400, and the last 200 steps are plotted in Figure 4. Although double periodicity and frequency-locking are illustrated by the sine-circle map in many literatures, the period-doubling bifurcation is also observed at $\alpha \simeq 0.6$ in Figure 4, which can make it easy to understand the similarity of the bifurcation structures between the sine-circle map and the Langford equation. The coexistence of two scenarios of routes to turbulence, quasi periodicity and period-doubling bifurcation, may be common in many of dynamical systems.

In order to study bifurcation structures of the Langford equation, sets of x_1 at its local maximum after transient states are plotted with various values of the parameter e . Eqs. (2-4) are solved by *NDsolve* command in *Mathematica* 5.2, which makes 100 to 500 different computations possible in a single program. The typical final time is $t_f = 2000 \sim 4000$ and the last period $t_f - t_d \leq t \leq t_f$ with $t_d = 200 \sim 600$ is picked up to identify attractors. In order to find the local maximum, the time period is divided into intervals with the width $\Delta t = 0.1$, and for the interval which can include the local maximum, the *FindMaximum* command is invoked. The typical initial condition for the numerical computation is $(x_1, x_2, x_3) = (0.01, 0, 0)$. We also choose the initial condition as the final state just before the parameter varied in order to examine the hysteresis. In some cases, multiple stable states are observed. About 40 different runs are performed with various regions of e and suitable numerical parameters.

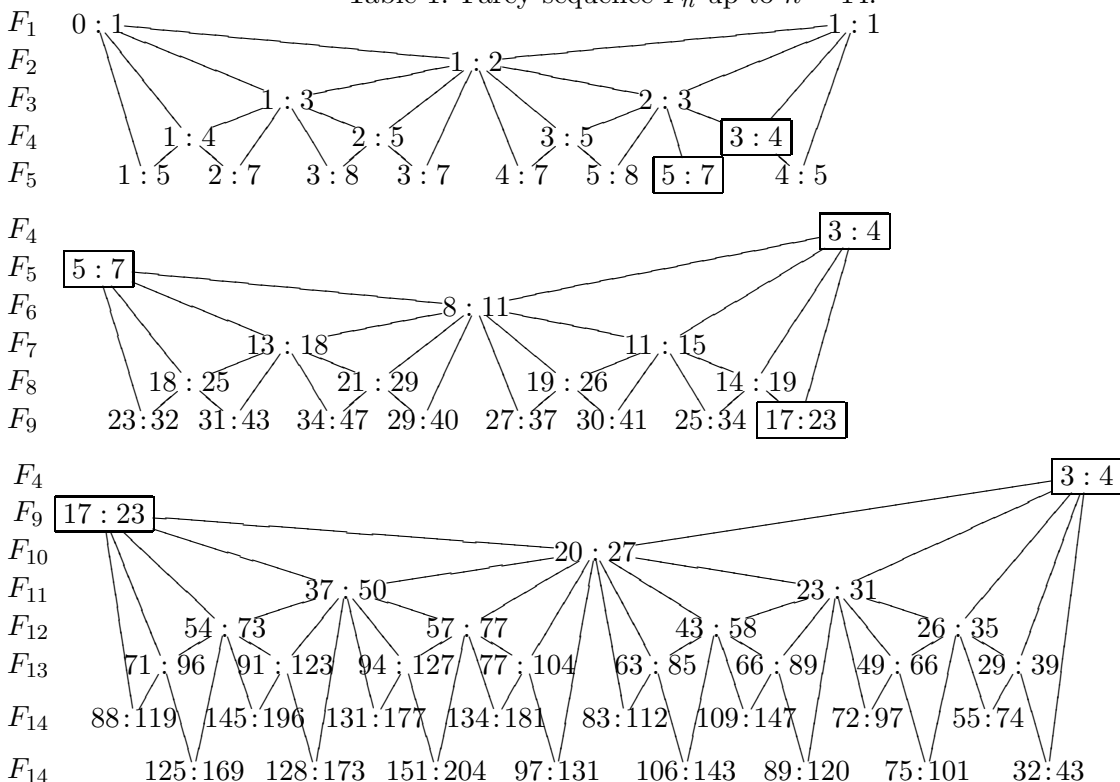
Figure 5 shows the bifurcation diagram for the parameter range $0 \leq e \leq 0.2$. The step of the parameter e is $\Delta e = 0.0001$. The region $e < 0.03$ includes doubly periodic solutions. Then 3:4 frequency-locking yields the periodic solution. The Feigenbaum period-doubling bifurcation occurs at $e \simeq 0.057$. There are many periodic windows as well as chaotic solutions after the period-doubling bifurcation. Its behavior is very similar to that of the one dimensional logistic map.

The range $0.02 < e < 0.03$ is enlarged in Figure 6, in order to see the most dominant frequency-locked periodic solutions. The solution is doubly periodic if $e < 0.02028$, even if e is negative. As e increases, a periodic solution with 17:23 resonance appears at $e \simeq 0.02028$. Periodic solutions shown by m_2 points are specified by the resonance condition $m_1 : m_2$ drawn at just below the upper frame of Figure 6. The region including double periodicity ends with the emergence of 3:4 resonance at $e \simeq 0.02935$. Doubly periodic solutions draw points whose numbers are controlled by the time range for plotting and typically much larger than the periodic solutions.

The Farey sequence F_n for integers $n > 0$ is the set of irreducible rational numbers a/b where $0 \leq a \leq b \leq n$ and the greatest common divisor of a and b is 1. The Farey sequence appears in frequency-locking of the sine-circle map. The resonance conditions between 17:23 and 3:4 are shown up to the Farey index $n = 14$ in Table 1.

For the 23:31 resonant periodic solution, an incomplete period-doubling bifurcation is ob-

Table 1: Farey sequence F_n up to $n = 14$.



served in Figure 6. Figure 7 shows the diagram enlarged for $0.021 < e < 0.0235$. Figure 8 shows the diagram for $0.0243 < e < 0.0253$. The period-doubling bifurcations observed on both of the two parameter regions of $43:58$ resonance.

The periodicity can be also judged by numerical computation of the square of the minimum distance

$$D = \min_{t>0} \sum_{i=1}^3 (x_i(t) - x_i(0))^2, \quad (10)$$

indicating the accuracy of recurrence. In Figure 9 for $0.0272 < e < 0.0283$, the small value of D indicates frequency-locked periodicity including resonances corresponding to $n = 15$ ($35:47$) and $n = 16$ ($38:51$ and $93:125$) of F_n .

The width of resonance decreases as the index n of F_n increases, that implies scaling laws as noted by [1]. Summary of observed stable periodic windows is given in Table 2. Figure 10 shows the parameter e versus the Farey index n for the periodic windows. Many of resonances $m_1 : m_2$ corresponding to Farey sequence F_n are confirmed, although some of them are not observed because of the possible lack of stability.

5 Conclusions

In conclusion, bifurcation structures similar to [1,2,8] is observed in the Langford equation; the coexistence of the double periodicity, frequency-locking and period-doubling bifurcations. The Langford equation would be one of the most illustrative ODE systems having double periodicity since it consists of only three variables. Each periodic attractor represents a corresponding knot in three dimensional space, as discussed in [3] for the Lorenz system and in [2] for the magnetoconvection system.

Recent progress of cost performance in computer hardware would make it possible to judge whether similar double periodicity and frequency-locking appear in the high dimensional Navier-Stokes turbulence and other chaotic systems. The method to judge quasi periodicity would be basically the same as that stated in the presented work.

This study was motivated by comments by Professor Bekki at the meeting of Japan Physical Society several years ago. The author is grateful to Professor Yamagata for support of research and to Professor Langford for sending the author his reprints.

References

- [1] N. Bekki and T. Karakisawa, Devil's Staircase in a Dissipative Fifth-Order System, *J. Phys. Soc. Jpn.* **69** (2000) 2443.
- [2] N. Bekki, Torus Knot in a Dissipative Fifth-Order System, *J. Phys. Soc. Jpn.* **69** (2000) 295.
- [3] L. H. Kauffman, *Knots and Physics*, Third Edition. World Scientific. (2001) 501.
- [4] W. F. Langford. Chaotic Dynamics in the Unfoldings of Degenerate Bifurcations, *Proceedings of the International Symposium on Applied Mathematics and Information Science, Kyoto University, Japan, March 29-31 (1982)*
- [5] W. F. Langford. A Review of Interactions of Hopf and Steady-state Bifurcations, *Nonlinear Dynamics and Turbulence, edited by G. I. Barenblatt, G. Iooss, and D. D. Joseph (1983)* 215.

- [6] W. F. Langford. Numerical Studies of Torus Bifurcations, *International Series of Numerical Mathematics* **70** (1984) 285.
- [7] D. Ruelle and F. Takens, On the Nature of Turbulence, *Communications in Mathematical Physics*, **20** (1971) 167.
- [8] M. Umeki, Bifurcations and Chaos in a Six-dimensional Turbulence Model of Gledzer, J. Phys. Soc. Jpn. **76** (2007) 043401.

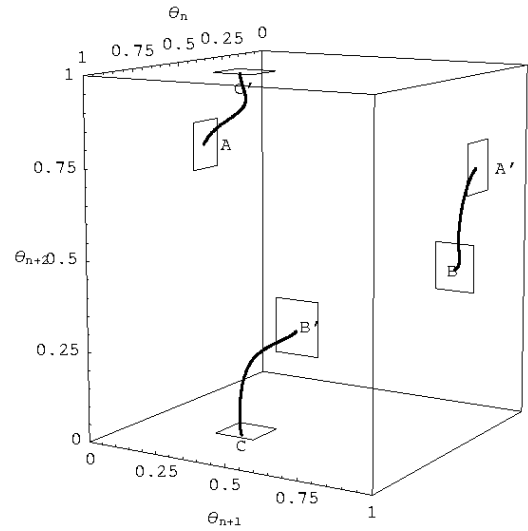
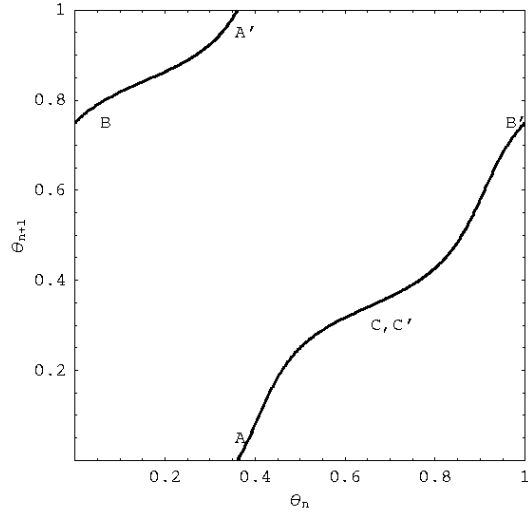
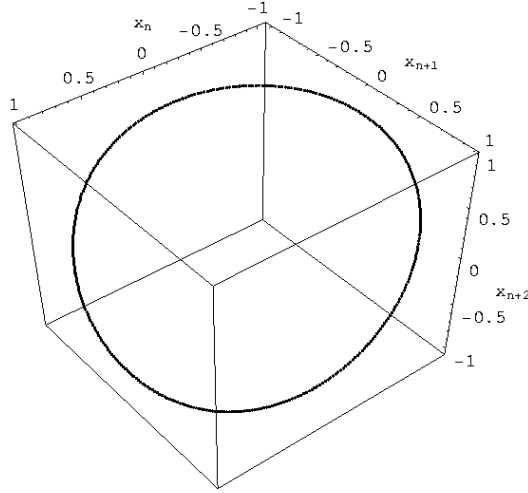


Figure 1: Poincaré plot of (1) for the double periodicity $a = 0$ in (a) the (x_n, x_{n+1}, x_{n+2}) space, on (b) the (θ_n, θ_{n+1}) plane, and in (c) the $(\theta_n, \theta_{n+1}, \theta_{n+2})$ space. Points A, B and A', B' in Figures 1(a) and 1(b), and C, C' in Figure 1(c), which are separated due to modulus 2π in the argument, are the same points. In order to see which surface the points lie on, the rectangles including the points are added in Figure 1(c).

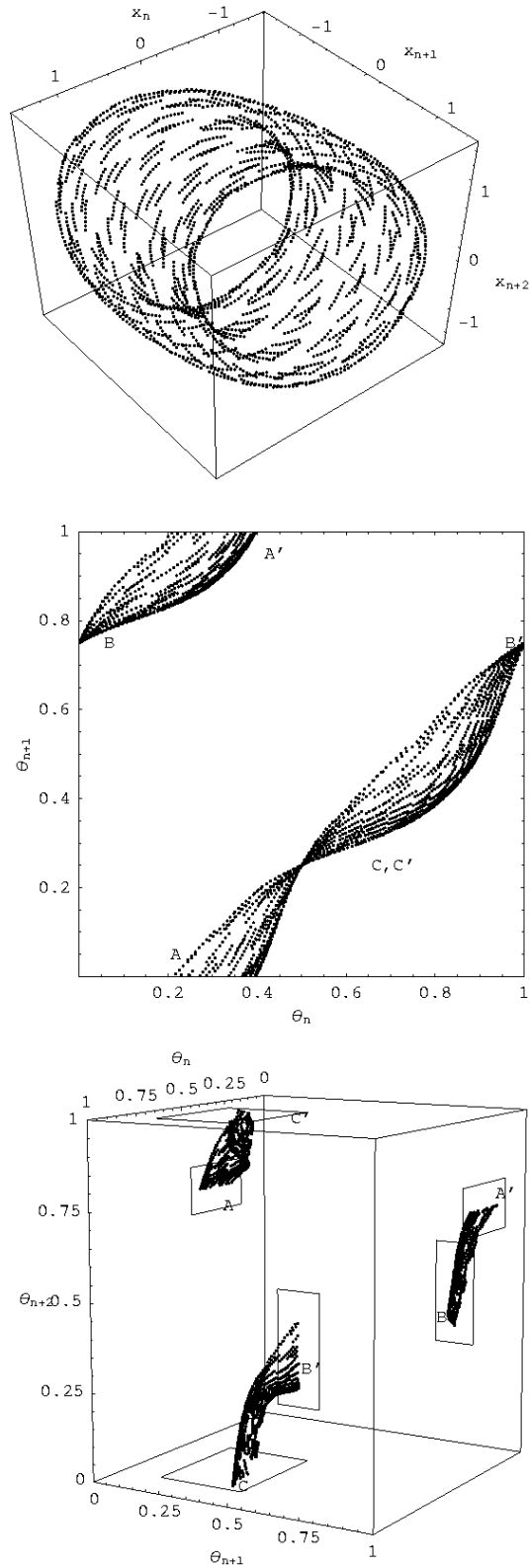


Figure 2: Poincaré plot of (1) for the triple periodicity $a = 0.5, \omega = \sqrt{2}$ in (a) the (x_n, x_{n+1}, x_{n+2}) space, on (b) the (θ_n, θ_{n+1}) plane, and in (c) the $(\theta_n, \theta_{n+1}, \theta_{n+2})$ space. The points are on the surface in Figure 2(a) and 2(c). As a in Eq. (1) increases, the width of the surface becomes large.

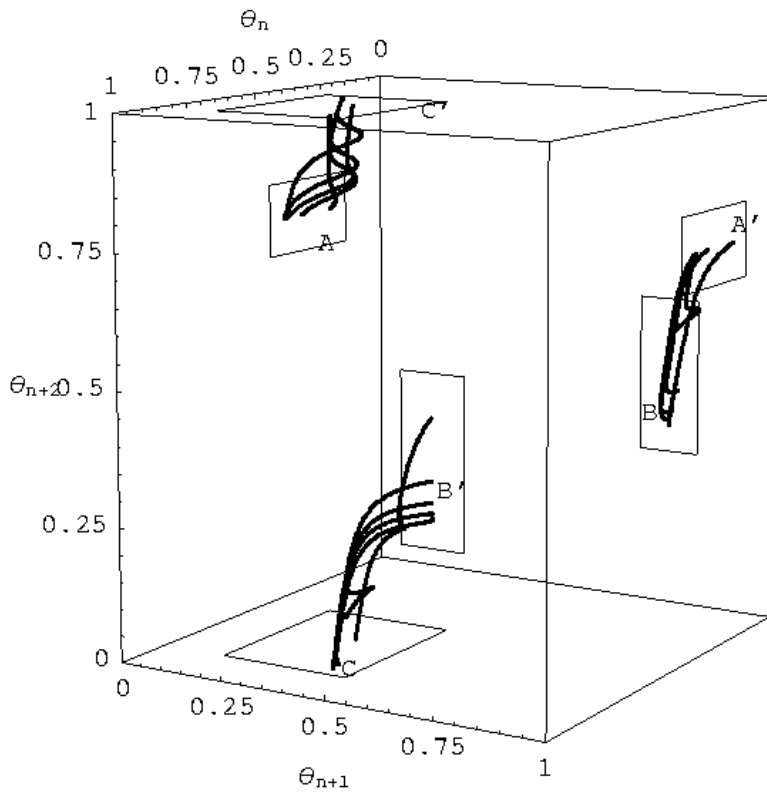
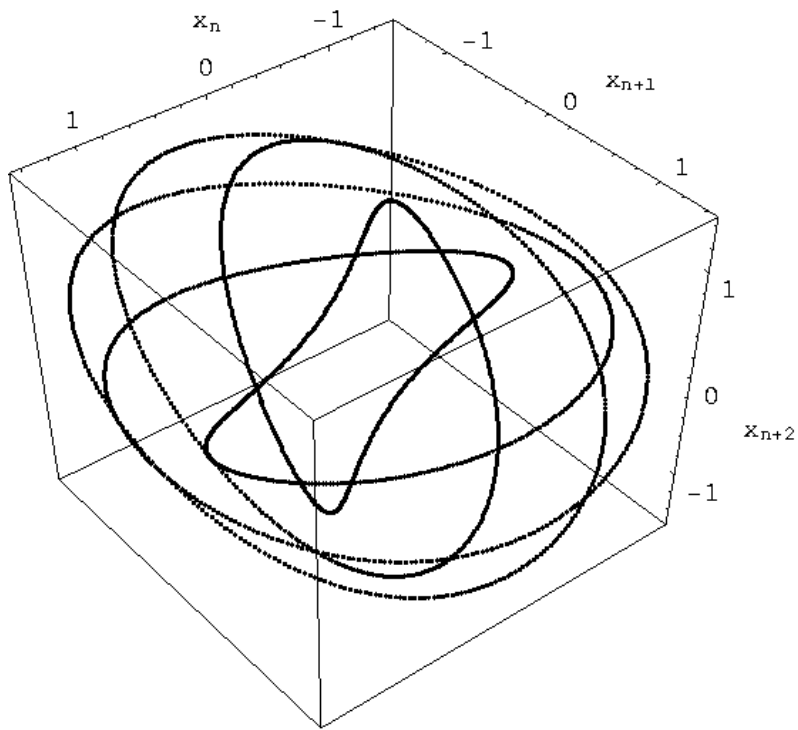


Figure 3: Poincaré plot of (1) for the frequency-locked double periodicity $a = 0.5, \omega = 1.4$ in (a) the (x_n, x_{n+1}, x_{n+2}) space and (b) the $(\theta_n, \theta_{n+1}, \theta_{n+2})$ space.

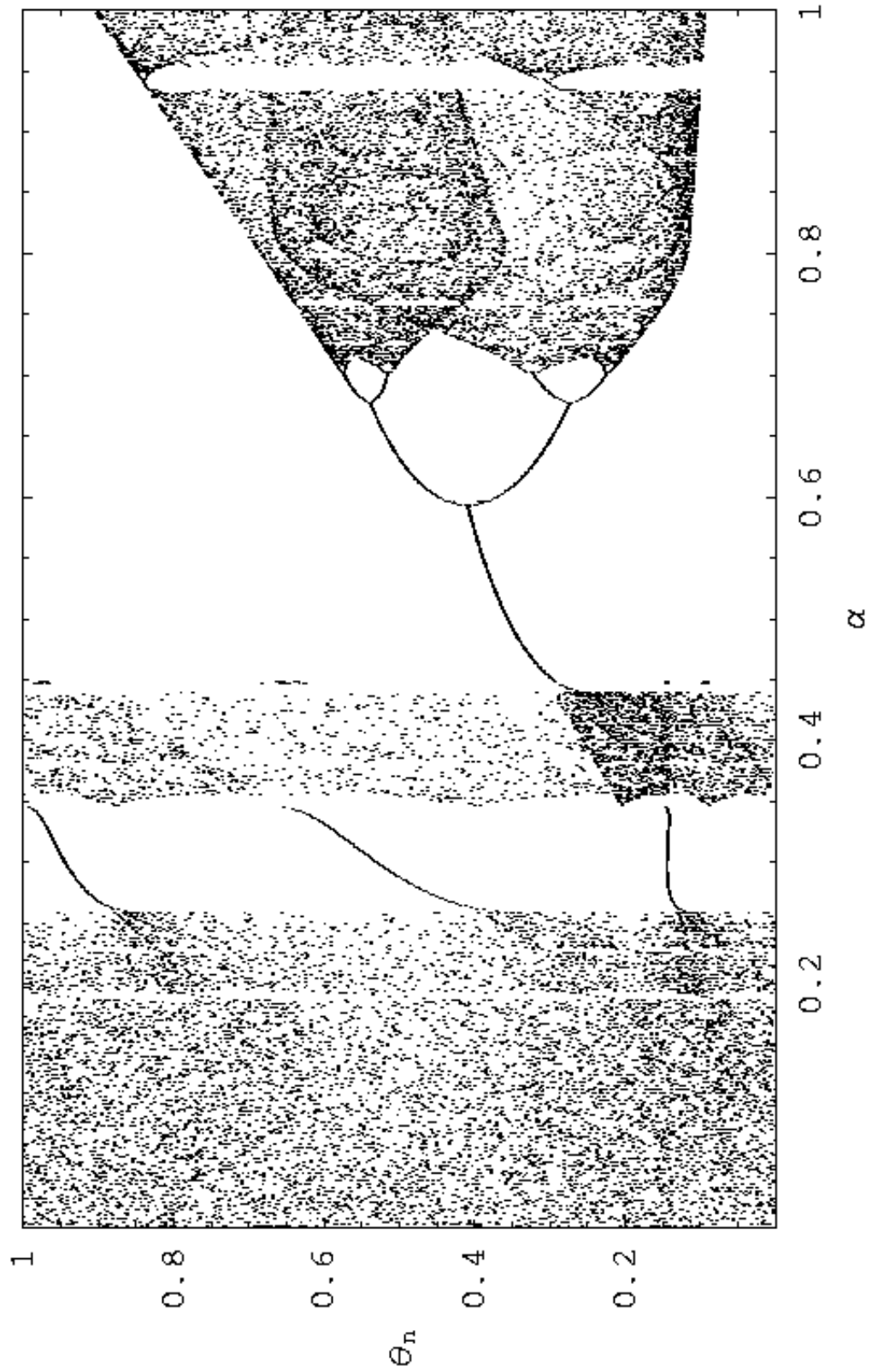


Figure 4: Bifurcation diagram of the sine-circle map (8). The parameters Ω and K are related as (9). 40000 points are randomly selected from the data for a clear view.

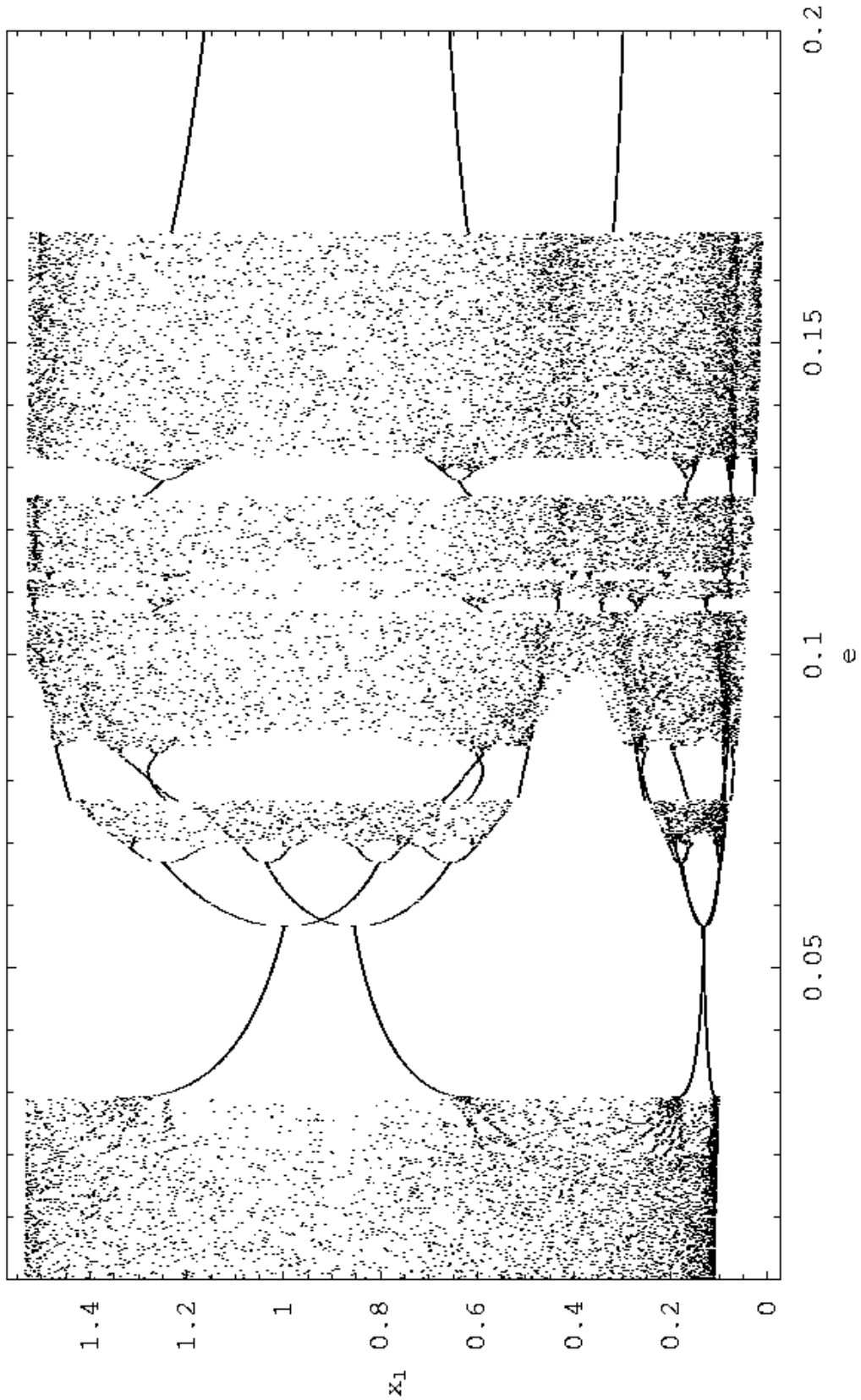


Figure 5: Bifurcation diagram of the Langford equation for $0 < e < 0.2$. 40000 points are randomly selected from the data for a clear view. In the following figures, bifurcation diagrams are for the Langford equation.

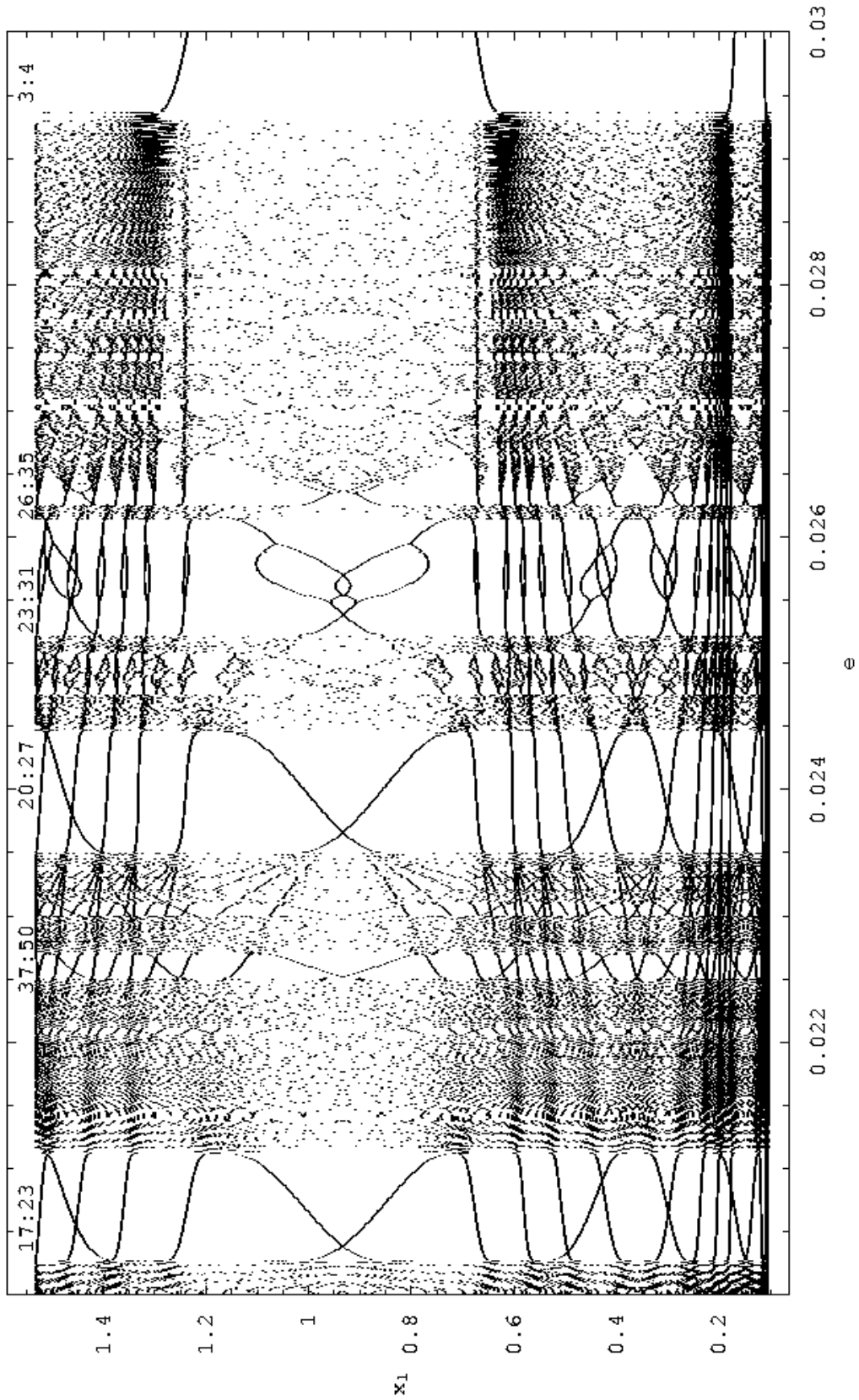


Figure 6: Enlarged bifurcation diagram for $0.02 < e < 0.03$.

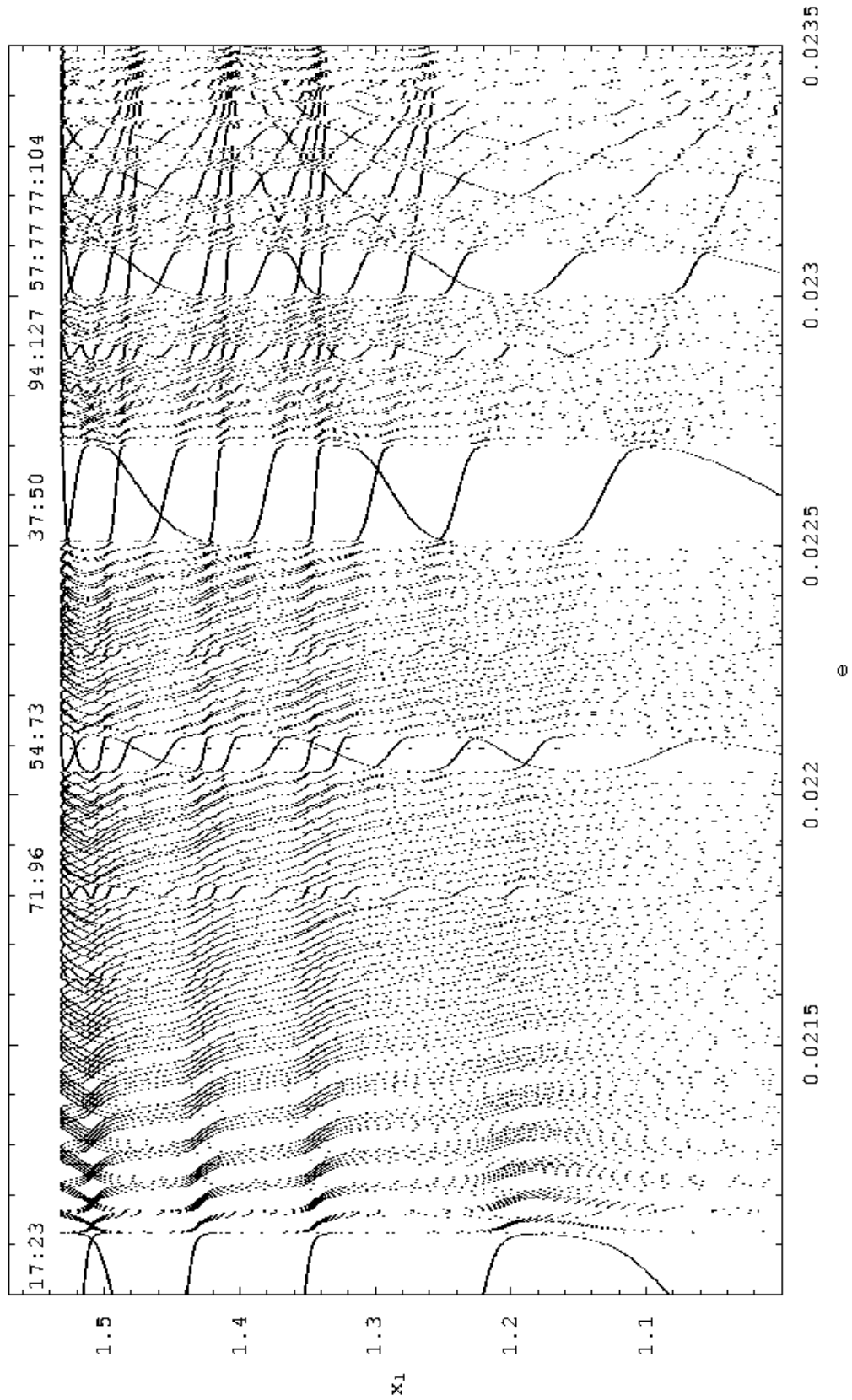


Figure 7: Bifurcation diagram enlarged again for $0.021 < e < 0.0235$.

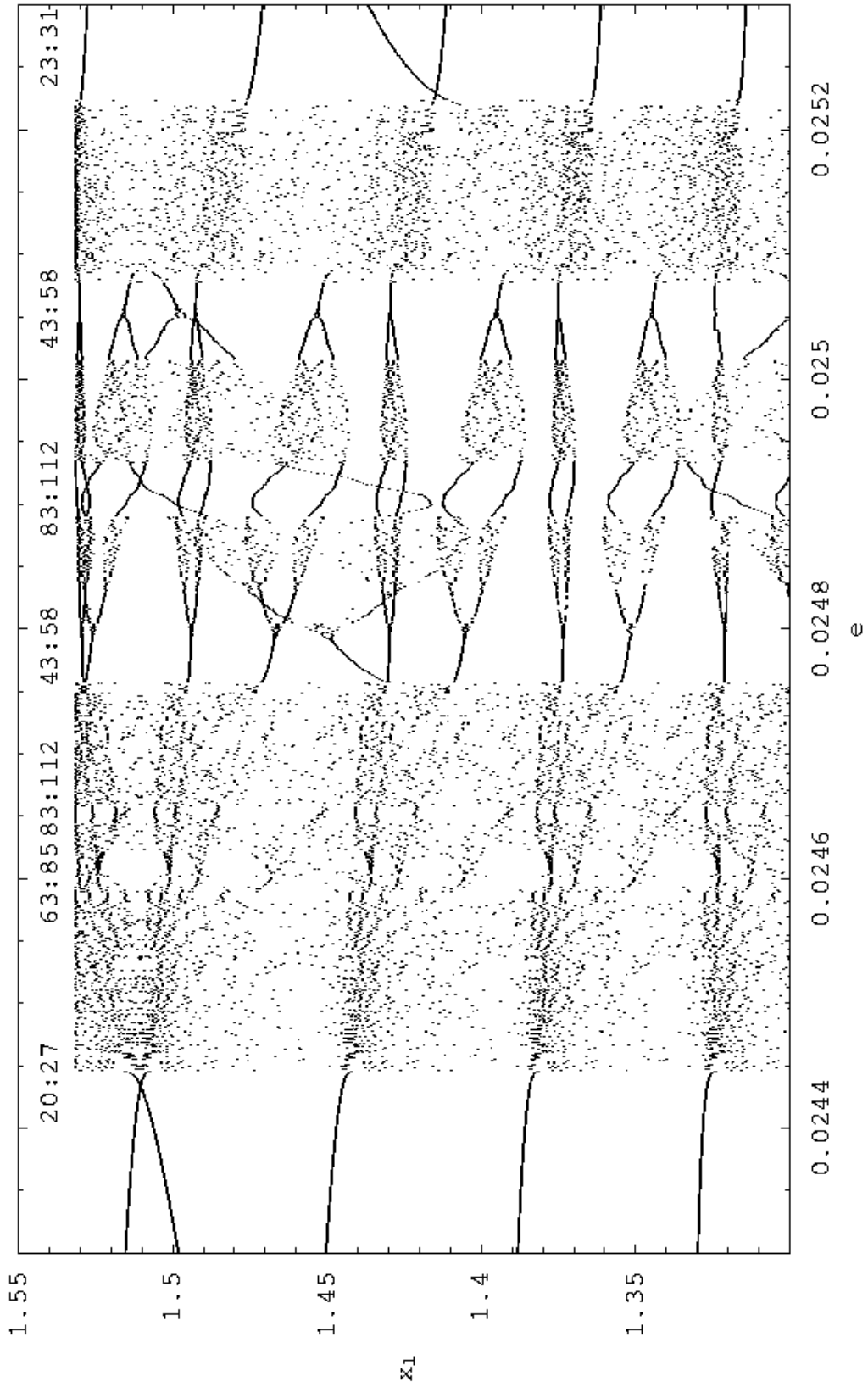


Figure 8: Enlarged bifurcation diagram for $0.0243 < e < 0.0253$. Two parameter regions for 43:58 and 83:112 resonances are observed. The period-doubling bifurcation follows from 43:58 periodic solutions.

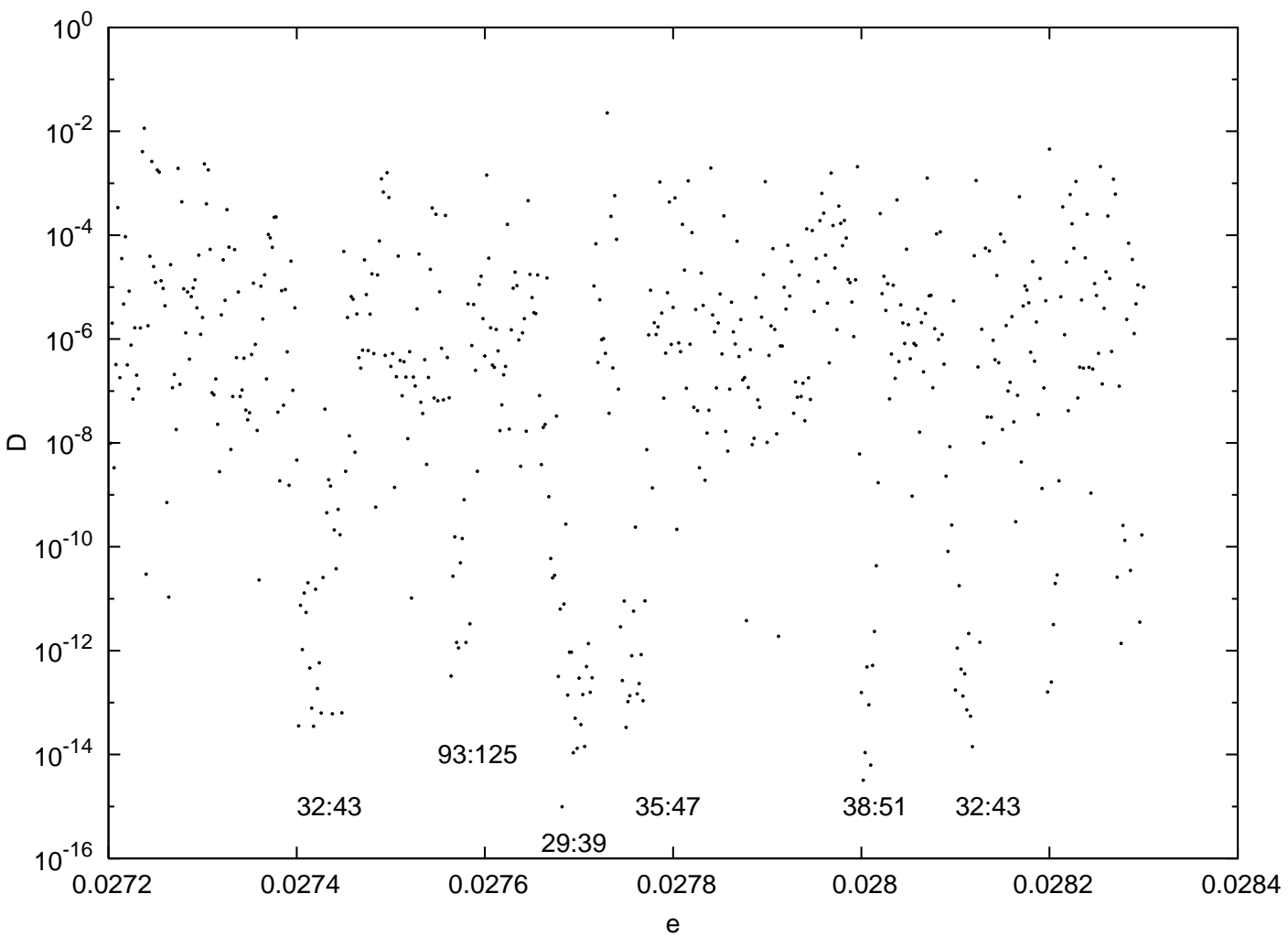


Figure 9: The parameter e versus the square of the minimum distance D of numerical solutions showing its accuracy of recurrence for resonant periodicity.

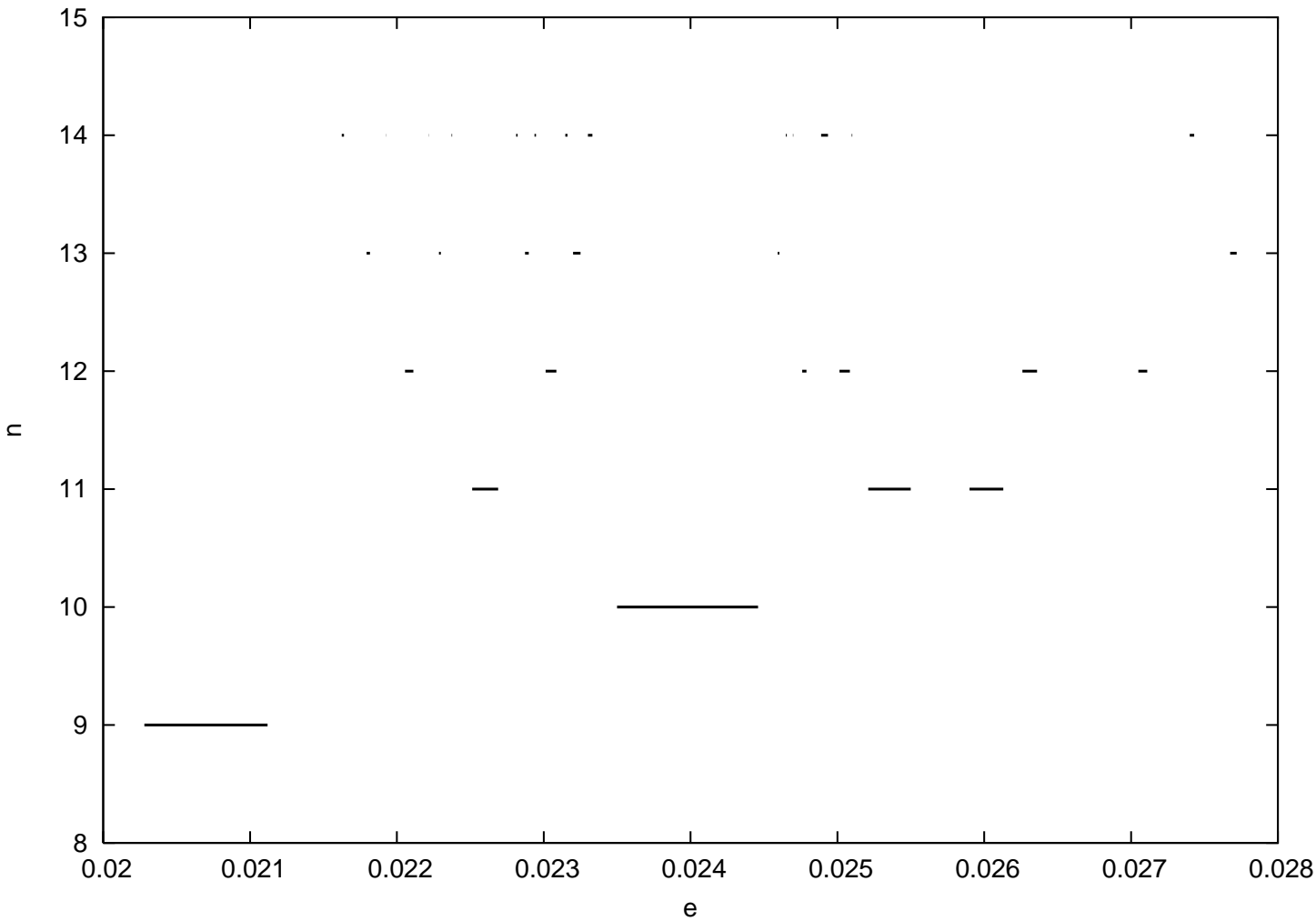


Figure 10: The parameter e versus the Farey index n for periodic windows.

Table 2: Observed periodic windows. $m_1 : m_2$ denotes the resonance condition, n the Farey index, and e_l (e_u) the lower (upper) limit of e , respectively. NF denotes that the resonant periodic solutions are not found.

$m_1 : m_2$	n	e_l	e_u
17:23	9	0.02028	0.02112
88:119	14	0.021625	0.021640
71:96	13	0.021794	0.021817
125:169	14	0.021924	0.021926
54:73	12	0.022056	0.022113
145:196	14	0.022217	0.022219
91:123	13	0.022287	0.022299
128:173	14	0.022373	0.022377
37:50	11	0.022513	0.02269
131:177	14	0.022813	0.022822
94:127	13	0.022873	0.022898
151:204	14	0.022937	0.022947
57:77	12	0.023013	0.023087
134:181	14	0.023147	0.023162
77:104	13	0.02320	0.023251
97:131	14	0.023301	0.023332
20:27	10	0.02350	0.02446
83:112	14	0.024650	0.024656
83:112	14	0.02489	0.0249356
63:85	13	0.024594	0.024605
106:143	14	0.024698	0.0247
43:58	12	0.02476	0.02479
43:58	12	0.025015	0.025085
109:147	14	NF	NF
66:89	13	NF	NF
89:120	14	0.025098	0.025102
23:31	11	0.02521	0.0255
23:31	11	0.0259	0.02613
72:97	14	NF	NF
49:66	13	NF	NF
75:101	14	0.0261475	0.026148
26:35	12	0.02626	0.02636
26:35	12	0.02705	0.02711
55:74	14	NF	NF
29:39	13	0.027675	0.02772
32:43	14	0.0274	0.02743
3:4	4	0.02935	0.057